MOUNTAIN-PLAINS CONSORTIUM

MPC 24-551 | Y. Wu, G. Hou, and S. Chen

RESILIENCE-BASED RECOVERY PLANNING OF TRANSPORTATION NETWORK FOLLOWING EARTHQUAKES

MOUNTAIN-PLAINS CONSORTIUM REGION 8

A University Transportation Center sponsored by the U.S. Department of Transportation serving the Mountain-Plains Region. Consortium members:

Colorado State University
North Dakota State University
South Dakota State University
University of Colorado Denver
University of Denver
University of Utah
Utah State University
University of Wyoming

Technical Report Documentation Page

1. Report No.	2. Government Accession No.	3. Recipient's Catalog No.
MPC-642		

4. Title and Subtitle	5. Report Date
Resilience-based Recovery Planning of Transportation Network Following Earthquakes	August 2024
	6. Performing Organization Code

7. Author(s)	8. Performing Organization Report No.
Yangyang Wu Guangyang Hou Suren Chen	MPC 24-551

9. Performing Organization Name and Address	10. Work Unit No. (TRAIS)
Colorado State University Department of Civil and Environmental Engineering Fort Collins, CO 80523	11. Contract or Grant No.

12. Sponsoring Agency Name and Address	13. Type of Report and Period Covered
Mountain-Plains Consortium North Dakota State University PO Box 6050, Fargo, ND 58108	Final Report
	14. Sponsoring Agency Code

15. Supplementary Notes

Supported by a grant from the US DOT, University Transportation Centers Program

16. Abstract

An efficient and safe transportation system is essential to communities during the long-term recovery period after earthquakes. A disrupted transportation network due to infrastructure damage or failure affects the functionality of the traffic system and poses increased traffic safety risks. A rational assessment of the traffic network performance in terms of both traffic efficiency and safety cannot only provide comprehensive quantification of system resilience, but also enable more risk-informed post-hazard recovery planning. A new methodology to assess the resilience performance of transportation networks during post-earthquake long-term recovery period is developed in this study with two main innovative contributions: (1) simulating the traffic performance of partially closed road segments in the network simulation and optimization, which offer useful tool to capture the time-progressive recovery process; and (2) integrating both traffic efficiency and safety into the resilience assessment and recovery prioritization. After a resilience indicator is introduced to characterize the overall traffic efficiency and safety of the transportation network using probabilistic sampling method, a comprehensive restoration priority measure is proposed to support post-earthquake restoration of damaged bridges. A demonstrative study is conducted on a hypothetical network system located in an earthquake prone area.

17. Key Word	18. Distribution Statement
disaster resilience, earthquakes, evaluation and assessment, infrastructure, network analysis (planning), traffic safety, transportation planning	Public distribution

19. Security Classif. (of this report)	20. Security Classif. (of this page)	21. No. of Pages	22. Price
Unclassified	Unclassified	35	n/a

Form DOT F 1700.7 (8-72) Reproduction of completed page authorized

RESILIENCE-BASED RECOVERY PLANNING OF TRANSPORTATION NETWORK FOLLOWING EARTHQUAKES

by

Yangyang Wu

Guangyang Hou

Suren Chen

Department of Civil and Environmental Engineering
Colorado State University
Fort Collins, CO 80523

August 2024

ACKNOWLEDGEMENT

The funds for this study were provided by the United States Department of Transportation to the Mountain Plains Consortium (MPC).

DISCLAIMER

The contents of this report reflect the views of the authors, who are responsible for the facts and the accuracy of the information presented. This document is disseminated under the sponsorship of the Department of Transportation, University Transportation Centers Program, in the interest of information exchange. The U.S. Government assumes no liability for the contents or use thereof.

ABSTRACT[1]

An efficient and safe transportation system is essential to communities during the long-term recovery period after earthquakes. A disrupted transportation network due to infrastructure damage or failure affects the functionality of the traffic system and poses increased traffic safety risks. A rational assessment of the traffic network performance in terms of both traffic efficiency and safety cannot only provide comprehensive quantification of system resilience, but also enable more risk-informed post-hazard recovery planning. A new methodology to assess the resilience performance of transportation networks during post-earthquake long-term recovery period is developed in this study with two main innovative contributions: (1) simulating the traffic performance of partially closed road segments in the network simulation and optimization, which offer useful tool to capture the time-progressive recovery process; and (2) integrating both traffic efficiency and safety into the resilience assessment and recovery prioritization. After a resilience indicator is introduced to characterize the overall traffic efficiency and safety of the transportation network using probabilistic sampling method, a comprehensive restoration priority measure is proposed to support post-earthquake restoration of damaged bridges. A demonstrative study is conducted on a hypothetical network system located in an earthquake prone area.

[1] This report is based on the contents from the published journal paper: Wu, Y., Hou, G. and Chen, S. (2021). "Post-earthquake resilience assessment and long-term restoration prioritization of transportation network", Reliability Engineering and System Safety, 211, 107612.

TABLE OF CONTENTS

LIST OF TABLES

LIST OF FIGURES

1. INTRODUCTION AND LITERATURE REVIEW

1.1 Background

Some disastrous natural hazards can cause severe structural damages, casualty, and injuries during very short time periods (Lu et al., 2019; and Liu et al., 2020). Following an earthquake, for example, some vulnerable transportation infrastructures such as bridges can be severely damaged, which may lose partial to full functionality. One example was during the 2008 Wenchuan earthquake when extensive highway and bridge damages were reported in Sichuan Province, China (Hu et al. 2014). The extensive repairs of disrupted transportation infrastructures usually take months or even years following earthquakes to finish, making the transportation network in the region remaining partially disrupted over an extended period during the long-term recovery stage (Blackman et al. 2017; Yi and Fu 2018). A timely recovery of a disrupted transportation network is of utmost importance because it cannot only help improving the traffic efficiency of the affected community, but also more importantly, expedite long-term recovery efforts of other critical infrastructures, e.g., buildings, power system and water system, that are heavily dependent on effective transportation. Moreover, partially disrupted traffic networks over extended durations of repairs will create multiple work zones with considerably elevated vehicle crash risks, threatening the safety of both general drivers and those involved in post-hazard recovery efforts (Yang et al. 2015). To strategically plan the long-term post-hazard recovery of disrupted transportation infrastructures requires rational performance modeling of disrupted transportation infrastructures and networks and consideration of both traffic efficiency and safety impacts.

There have been a long history of studies focusing on the post-disaster performance modeling of transportation networks (e.g., Kozin and Zhou 1990; Wakabayashi & Kameda 1992; Chang and Nojima 2001; Zamanifar & Seyedhoseyni 2017; and Sun et al 2020). Some studies paid attention to the resilience analysis and modeling of critical transportation infrastructures. Akiyama et al. (2020) investigated the importance of considering both independent and interrelated hazards on bridges by developing a life-cycle reliability and risk approach to assess bridge and networks under both independent and interaction hazards like earthquakes, tsunami, and corrosion. Dong & Frangopol (2015) estimated the risk and resilience of bridges under earthquakes by proposing an approach to improve bridge mitigation under seismic hazard. Besides the mainshocks, they also investigated the impact of aftershocks on the bridge resilience, and concluded aftershocks have significant effects on bridge repair loss and residual functionality. Argyroudis et al. (2020) proposed an integrated framework to account for the nature and sequence of multiple hazards and their effects and to quantify the resilience of critical transportation infrastructures subjected to hazards considering the structural vulnerability and recovery rapidity. Some other studies estimated the transportation network resilience based on connectivity and accessibility of the network. Zhang & Wang (2016) proposed the weighted independent pathway as the network performance metric to systematically integrate the network topology and roadway redundancy level. Wu & Chen (2019) modeled the resilience performance of traffic network in terms of the accessibility of medical resources during the emergency medical response period considering the interactions between transportation infrastructures, people and hazard. Zhou et al. (2019) proposed the concepts of "global connectivity" and "local connectivity" to consider both the connection extent of the whole transportation network and the distance between each node to its neighbors and evaluated the system efficiency using percolation theory. In recent years, more and more researchers incorporated travel demand and traffic assignment methods into their works when simulating the resilience and performance of transportation networks during post-earthquake period. Alipour & Shafei (2016) proposed a comprehensive framework to quantify the seismic resilience of the transportation networks considering the degradation in the functionality of the network caused by bridge damages and the effect of aging mechanisms of bridges and demonstrated the approach on the highway network of Los Angeles and Orange Counties. Kilanitis & Sextos (2019) developed a framework to estimate the comprehensive loss of the transportation networks

caused by travel time variations and trip cancelations and simulated the variation of origin-destination demand during the post-earthquake recovery period. Kameshwar et al. (2020) developed a bridge restoration model based on decision trees to assess the performance of regional road networks under extreme events to provide a detailed assessment of bridge functionality and traffic restriction and derived the traffic capacity of disrupted links based on the Highway Capacity Manual. Although they proposed a methodology to assess various functional levels of bridge and road and adopted the traffic assignment method to derive the performance index based on travel time and distance, they didn't consider the traffic safety and the impact of road disruption on other parameters in the Bureau Public Road function beyond link traffic capacity.

In addition to studies focusing on post-hazard traffic performance assessment, there have also been some studies focusing on post-hazard restoration planning and bridge prioritization. Most of the studies optimized the post-earthquake restoration based on the network performance or resilience and information about infrastructure repair time, limited resources, and contractors (e.g., Chen and Tzeng 1999; Cho et al., 2000; Orabi et al., 2009, 2010; and El-Anwar et al., 2015). Bocchini & Frangopol (2012a) presented an optimization for the repair activities of the bridges in a transportation network that are severely damaged by an earthquake. The study adopted three conflicting objectives: maximizing network resilience, minimizing the time and total costs, and provided an entire set of Pareto solutions to the optimization. Bocchini & Frangopol (2012b) built a model to prioritize the intervention of bridges along a highway segment by incorporating both travel time and distance into the resilience indicator and conducting the optimization with two conflicting objectives: resilience and cost. Zhao & Zhang (2020) proposed a bi-objective and bi-level optimization framework to optimize the transportation infrastructure restoration plan. They took the unmet demand and total travel time as performance measures and solved the optimization using elastic user equilibrium and a modified active set algorithm. Although these studies optimized the bridge restoration based on network performance including incorporating network performance, limited resources, and traffic assignment, they didn't consider the effect of work zones on travel time, safety, and bridge prioritization. Most existing studies investigated the bridge and link importance, or prioritization based on the network connectivity, accessibility, and topology. Wu & Chen (2019) defined the importance value for vulnerable links based on their impact on the network performance by comparing the network performance when a link works or fails. Stochastic method wasn't employed because the uncertainty was considered using the occurrence probability for each scenario. Merschman et al. (2020) prioritized the bridge repair using three performance measures: total travel distance and time, bridge importance based on connectivity, and a social measure in terms of the accessibility to emergency facilities. The bridge importance measure is defined from the topology of the network and shortest paths. These studies focused mainly on the post-hazard emergency response stage, and the proposed connectivity-based bridge importance measures cannot be applied to bridge restoration planning. A very limited number of studies considered the partial functionality of links when deriving bridge prioritization. Wang & Jia (2019) proposed an efficient sample-based approach to estimate a probabilistic sensitivity measure of the network that yields bridge importance rankings for pre-earthquake risk mitigation priorities. The methodology incorporated the uncertainties in hazards and bridge damage states and enabled effective search of the mitigation strategies within a small subset. Also. They considered the partial functionality of disrupted links by assuming different levels of capacity according to damage states. Liu et al. (2020) also considered the reduced traffic carrying capacity of damaged links and proposed a modified network robustness index as the resilience measure to prioritize the network recovery using a two-stage optimization method. The traffic capacities of damaged links were assumed to be determined through communication with stakeholders. Both studies considered partial functionality of damaged links, but the remaining traffic capacity was not rationally assessed or investigated.

All these studies as summarized above have made important contributions to the post-disaster traffic performance assessment and reconstruction planning during the long-term recovery stage. There are, however, still several major limitations: (1) most of the studies considered either fully closed or fully

opened links in terms of the functionality of traffic networks following hazards. As discussed earlier, the restoration processes of infrastructures (e.g., severely damaged bridges or roads) following earthquakes usually take rather long time. It is very common that some roads or bridges may only remain open for some lanes for certain time periods, especially given the common shortage of available restoration resources. Assumptions of instantaneous repair and recovery made in many existing studies were not realistic, which directly affect the accuracy and rationality of related traffic performance assessment and prioritization decisions during the long-term recovery stage. Although some studies have related the bridge traffic restrictions to the bridge functionality levels based on the Highway Capacity Manual (Kameshwar et al. 2020), they didn't consider the effects of bridge length and flow merging and diverging on link travel time, which are very important when simulating the traffic performance of partially closed links. A methodology to rationally assess the traffic performance on transportation networks with various levels of disruptions between fully closed and fully opened is still lacking; (2) as discussed earlier, a partially disrupted transportation network (e.g. bridges and roads with limited lanes open) not only affects travel time, but also creates multiple work-zone scenarios and results in merging and diverging of link traffic flows, which considerably increase vehicle crash risks (Yang et al. 2015). Therefore, for traffic planning in the long-term recovery stage following earthquakes, both travel time and safety risks should be appropriately considered for partially disrupted traffic networks; (3) uncertainties associated with hazards and bridge fragility affect the long-term recovery stage, which have been rarely incorporated into the existing studies of traffic performance (e.g. time and safety). In addition, post-disaster repair priority of the vulnerable bridges is related not only to the network topology and infrastructure location but also to the seismic uncertainty, travel demand, traffic efficiency and safety. So, for the traffic performance assessment and post-disaster restoration prioritization, uncertainties should be carefully incorporated.

1.2 Organization of This Report

This study aims to address these gaps by proposing a methodology to assess the resilience performance of transportation networks during the post-earthquake long-term recovery period that can consider the traffic performance of roads with partially functioning bridges. The resulting resilience framework can provide reliable information on travel time and traffic safety of roads with closed lanes on their bridges. This study uses a microscopic traffic flow simulation model (Hou et al. 2017, 2019) to simulate road travel time so it can be used to any road with given parameters and lane closure conditions. Moreover, this study adopts statistical methods for transportation data analysis to estimate the traffic accident frequency of roads with different bridge functionality levels and it can be applied to different roads if given the site-specific traffic crash data (Washington et al. 2010). A resilience indicator is proposed based on the simulated travel time and traffic safety performance to evaluate the performance of regional road networks after major hazards. The model uses existing seismic attenuation laws and bridge fragility data to estimate bridge failure, applies Monte Carlo simulation and Latin Hypercube sampling to consider the uncertainties in earthquake intensity and bridge fragility, and adopts User-Equilibrium (UE) method (Wardrop 1982) and Frank-Wolfe algorithm (Frank & Wolfe 1956; Janson 1991; and Lee & Machemehl 2005) to conduct traffic assignment. Furthermore, this study proposes a bridge restoration prioritization measure based on system resilience and uncertainties to provide critical information for stakeholders to make risk-informed decisions on bridge restoration during post-earthquake long-term recovery period. The Greedy algorithm and probabilistic sampling method are adopted to derive the bridge prioritization measure. The proposed methodology is applied to the transportation network of Centerville (Ellingwood et al. 2016), a hypothetical community located in an earthquake prone area.

The report is composed of four chapters: Chapter 1 introduces pertinent background information and literature review results related to the present study. In Chapter 2, the resilience assessment framework of disrupted traffic network in long-term recovery stage is introduced. In Chapter 3, numerical demonstration of the proposed framework through case study is conducted. Chapter 4 summarized the findings from the report, followed by some discussions.

2. RESILIENCE ASSESSMENT FRAMEWORK OF DISRUPTED TRANSPORTATION NETWORK IN LONG-TERM RECOVERY STAGE

The objective of this study is to assess the resilience performance of transportation networks during post-earthquake long-term recovery period, incorporate travel efficiency and safety of disrupted roads and propose a bridge prioritization measure to support decision makings on post-earthquake bridge restoration. As shown in Figure 2.1, the methodology starts with hazard simulation to generate bridge damage scenarios. The input data includes earthquake information like Richter magnitude, location of the epicenter, and locations of the bridges; and the output are the earthquake intensities like peak ground acceleration. Seismic attenuation laws and probabilistic sampling methods are applied to estimate earthquake intensities and their uncertainties, respectively. Then the sampled earthquake intensities are used to generate possible bridge damage scenarios based on bridge seismic fragility and probabilistic sampling method.

In Figure 2.1, when simulating the travel time of roads with different levels of functionalities, the inputs are the road and traffic information. Methods like microscopic traffic flow simulation can be adopted to derive the modified Bureau of Public Road function (US Bureau of Public Roads 1964) to accommodate partial functionality of roads due to bridge damages. For any sampled bridge damage scenario and given travel demand, the travel time and traffic flow of the links and the system can be estimated using traffic assignment methods. For the long-term recovery period, the traffic demand of the system can be recovered to almost the same as the pre-disaster level, and the travel demand of each OD pair can usually be obtained from the transportation department of a city (Chang et al. 2012) or estimated from existing Metropolitan Planning Organization (MPO) models (Kimley-Horn et al., 2007). So, it is assumed in this study the travel demand of the community during the long-term recovery period is same as the pre-earthquake level. The traffic flows of different links, together with other traffic safety factors, such as work zone lengths, are the inputs when deriving the traffic safety model using regression models like Poisson regression and Negative Binomial regression (Washington et al. 2010). The total system crash frequency for any sampled scenario can be estimated with the traffic safety model and link traffic flows.

In this study, the resilience index is defined based on the total system travel time and total system crash frequency (Figure 2.1) to consider both the traffic efficiency and safety performance of the transportation network. By introducing the level-of-performance (LOP) criterion, the system reliability is derived through quantifying the number out of the sampled scenarios under which the performance of the transportation network, in terms of travel time and traffic safety, can meet the selected criterion. The bridge restoration prioritization measure is the indicator for the decision-makers to prioritize the bridge restoration, especially when only limited resources are available. The detailed process and information of the proposed methodology are presented in the following sub-sections.

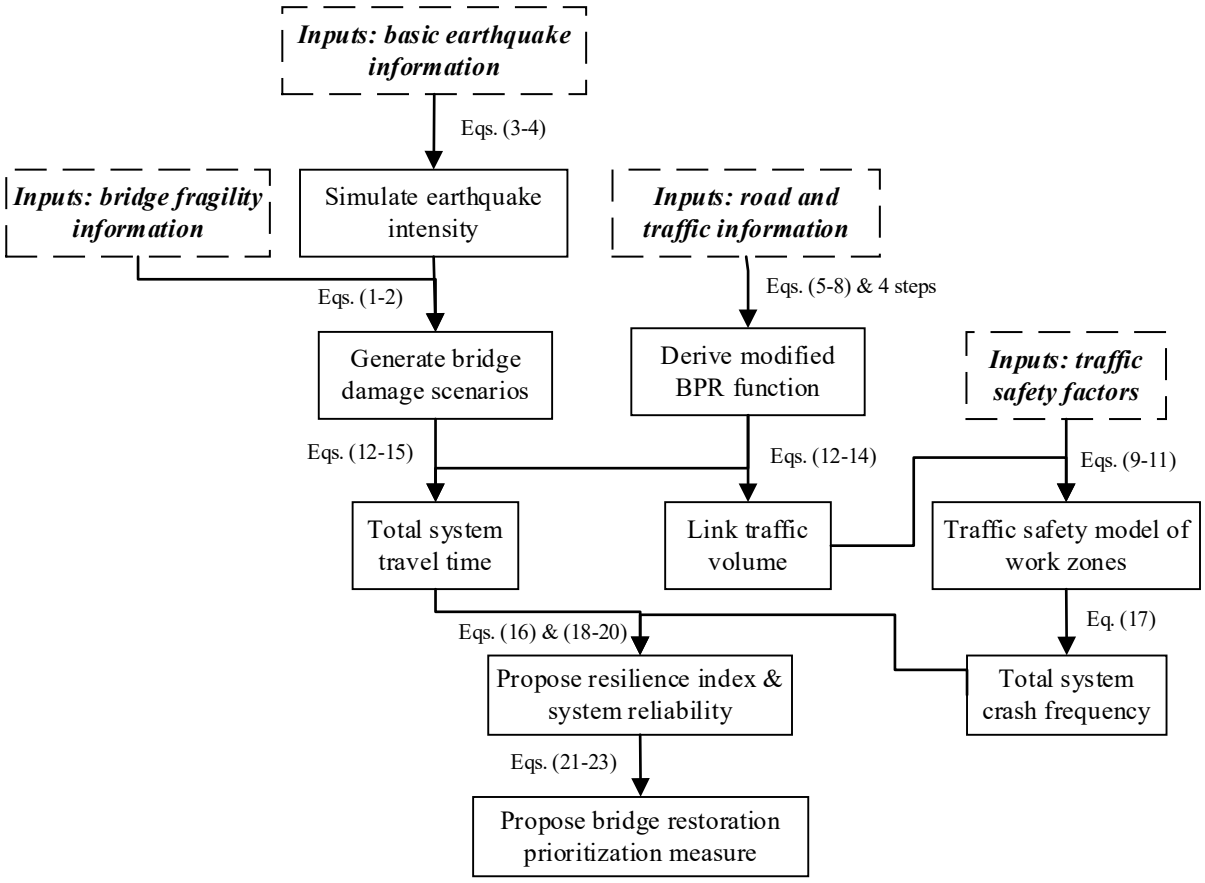

Figure 2.1 Flowchart of the model

2.1 Seismic Fragility of Bridges

The seismic fragility of structures can be defined as the probabilities of a given failure type of the structure under a given intensity level of earthquakes, e.g., spectral acceleration (SA). The failure in terms of a limit state is defined as an excess of the limiting value of the performance indicator, such as stress, displacement, or others. There are many sources of uncertainties affecting the accuracy of the structural capacity and fragility curves are often used to quantify the confidence level for each damage or limit state. For bridge seismic analyses, typically there are several different damage states, for example, no damage or slight/minor damage, moderate damage, extensive damage, and complete damage (Nielson & DesRoches 2007, and Argyroudis et al., 2019). For each damage state, the fragility curve stands for the probability of occurrence under different values of a hazard parameter. The probability of a bridge suffering and exceeding a given damage state is modeled as a cumulative lognormal distribution. For bridge damage, given the peak ground acceleration, PGA, the probability of suffering or exceeding a damage state, i, is modeled as:

$$P[Damage\ State\ i\ or\ greater|PGA] = \Phi\left[\frac{\ln(PGA)-\ln(med_i)}{\zeta_i}\right] \quad (1)$$

where med_i is the median PGA value of damage state i; ζ_i is the dispersion of damage state i (Nielson & DesRoches 2007). The damage state of bridge i is defined as:

$$D_i = D_i\left(PGA\left(\xi_p\right), \xi_{di}\right) \quad (2)$$

where ξ_p is the uncertainty of PGA; ξ_{di} is the uncertainty of structural damage in the fragility curve of bridge i (Chang et al., 2012).

PGA is one of the commonly used seismic intensities when developing seismic fragility of bridges (e.g., Nielson & DesRoches 2007), so it is adopted herein to estimate the bridge damage states in this study. The median of the peak ground acceleration, $\overline{PGA}$, of a given location can be derived by the attenuation laws in terms of Richter magnitude (M_L) and epicentral distance (R_e).

$$\overline{PGA} = f(M_L, R_e) \tag{3}$$

The uncertainty of PGA is often assumed to follow a lognormal distribution because the seismic ground motions are estimated with attenuation laws that are usually modeled as the exponential of M_L and R (Campbell 1981). PGA at a given location follows lognormal distribution:

$$\ln PGA = \ln\left(\overline{PGA}\right) + \xi_p \tag{4}$$

where ξ_p is the uncertainty of PGA, same as in Eq. (2). Following the work by Adachi and Ellingwood (2007), PGA is assumed with a coefficient of variance of 0.6.

2.2 Travel Time Estimate on Post-earthquake Urban Arterials

2.2.1 Post-earthquake Traffic on Urban Arterials

In post-earthquake urban transportation networks, road links may be disrupted directly or indirectly. In this study, we only consider the disruption to the traffic flow by damaged bridges given the fact that other temporary or relatively minor disruptions are reasonably assumed to be completed by the time of long-term recovery. According to Padget and DesRoches (2007), a moderately or less damaged bridge can typically be recovered to its original traffic carrying capacity one week after the earthquake, while an extensively damaged bridge can only recover 50% of its capacity while a completely damaged bridge cannot carry any traffic. Considering the long-term recovery period usually begins at least 7 days after the earthquake, the traffic capacity from the survey by Padget and DesRoches (2007) still can be applied during long-term recovery periods. When site-specific data of traffic capacity of damaged bridges is not available, the generic data from the existing studies (e.g., Padget & DesRoches 2007) will be adopted.

For demonstration purposes in this study, a bridge which cannot carry any traffic (completely damaged) is deemed to be totally closed; and 50% traffic carrying capacity (extensively damaged) is assumed that half of the lanes are closed on the bridge. This study focuses on urban transportation networks with two-way single-lane and two-way double-lane roads, which are very common in the US. If a bridge on any of the two-way single-lane roads suffers complete damage, the road will be closed to all the through traffic. If a bridge on a two-way single-lane road suffers extensive damage, it is assumed one of the lanes on the bridge will be closed as a "work zone" and the other lane will accommodate traffic with a flag person to direct the traffic of the lane. In this case, it is assumed the free flow travel time on this link is doubled while the capacity remains the same. If a bridge on a two-way double-lane road suffers extensive damage, two lanes on the bridge will be closed as "work zones" and the link will be degraded into a partial two-way single lane road with "work zones". Therefore, for an urban transportation network with two-way single-lane and two-way double-lane roads, there are three typical traffic scenarios after earthquakes (Figure 2.2): the first one is the normal 1-lane traffic, the second one is the normal 2-lane traffic, and the

third one is the disrupted 2-lane traffic, in which one lane is closed for the damaged bridge and the other lane is open.

(a) Normal 1-lane traffic

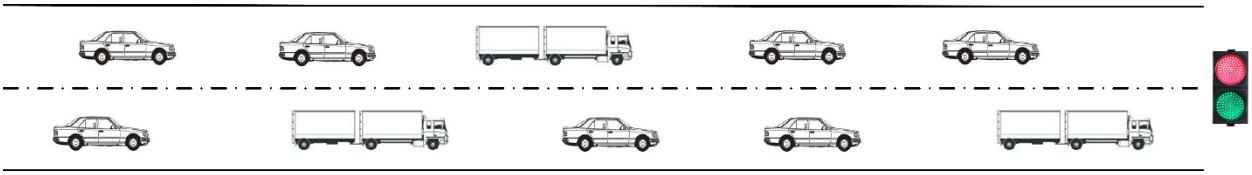

(b) Normal 2-lane traffic

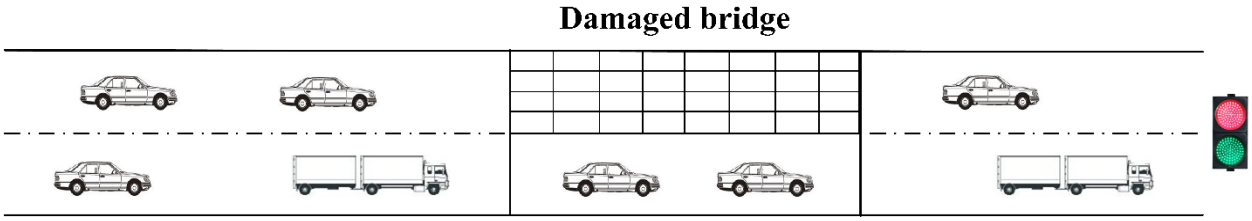

(c) Disrupted 2-lane traffic

Figure 2.2 Post-earthquake traffic scenarios

2.2.2 Microscopic Traffic Flow Simulation Model

For intact roads shown in Figure 2.2 (a) and (b), the travel time on a road link has been often predicted with the widely adopted travel time functions for intact roads (e.g., BPR functions). Lane reduction due to damaged bridges shown in Figure 2.2(c) will reduce the road traffic capacity and increase the travel time. For roads with partial disruptions as shown in Figure 2.2(c), the corresponding travel time functions are however not available and therefore need to be defined before the traffic performance can be assessed quantitatively. Traditionally, travel time function for intact roads can be established based on empirical data from traffic monitoring or calibrating the coefficients of BPR functions. Actual post-hazard traffic data, however, has been very rare and as a result, simulation-based approach is often needed to derive the travel time functions for various disruption scenarios. In this study, a Cellular Automaton (CA)-based microscopic traffic flow simulation model developed by Hou et al. (2017, 2019) is used to simulate normal and disrupted traffic flow on post-earthquake arterials and estimate the travel time functions.

The effect of traffic lights must be considered for urban arterials. As shown in Figure 2.2, there is a traffic light at the right end of a road section, with a cycle length of T and a green ratio of R. The orange light period is ignored. The durations of green-light phase and red-light phase are $T_g = T * R$ and $T_r = T - T_g$, respectively. The CA model used in this study includes forwarding and lane-changing rules. The longitudinal position and velocity of vehicle i are denoted by x_i^t and v_i^t at the time step t. At next time step $t + 1$, position x_i^{t+1} and velocity v_i^{t+1} can be updated through the forwarding and lane-changing rules. The forwarding rules can be described as a process of step 1 to 4, which are performed in parallel for all the vehicles.

Step 1 Acceleration: $v_i^{t+1} = min\left(v_i^t + a_i, v_{i,max}\right)$.

Step 2 Deceleration: $v_i^{t+1} = min\left(v_i^{t+1}, gap_i^t\right)$, if the traffic light is green in front of vehicle i; $v_i^{t+1} = min\left(v_i^{t+1}, gap_i^t, S_i\right)$, if the traffic light is red in front of vehicle i.

Step 3 Randomization with a probability of p_r: $v_i^{t+1} = max\left(v_i^{t+1} - d_i, 0\right)$.

Step 4 Movement: $x_i^{t+1} = x_i^t + v_i^{t+1}$.

where $v_{i,max}$ denotes the maximum velocity of vehicle i; a_i and d_i denote the acceleration rate and deceleration rate of vehicle i; gap_i^t is the clear distance between vehicle i and its front vehicle $i+1$ on the current lane at time step t, $gap_i^t = x_{i+1}^t - x_i^t - l_i$; l_i is the length of vehicle i; S_i is the clear distance between vehicle i and the traffic light.

For 2-lane traffic as shown in Figure 2.2(b) and (c), vehicle i will perform a lane-changing maneuver with a probability of p_{ch}, if the lane-changing rules shown in Eq. (4) to (6) are satisfied.

$$gap_i^t < min\left(v_i^t + a_i, v_{i,max}\right) \tag{5}$$

$$gap_{i,f}^t > gap_i^t \tag{6}$$

$$gap_{i,b}^t > v_{i,b}^t \tag{7}$$

where $gap_{i,f}^t$ is the clear distance between vehicle i and the nearest vehicle on the target lane ahead of vehicle i at time step t; $gap_{i,b}^t$ is the clear distance between vehicle i and the nearest vehicle on the target lane behind vehicle i at time step t; $v_{i,b}^t$ is the velocity of the nearest vehicle on the target lane behind vehicle i.

Open boundary conditions are used in this model. Vehicles are injected into the road section of simulation from the left end with a flow rate of q, and the time headway h is assumed to follow a displaced exponential distribution, which has a cumulative probability distribution as follows:

$$F(h) = 1 - e^{-\lambda(h - t_m)} \tag{8}$$

where $F(h)$ is the cumulative distribution function of h; t_m is the minimum headway between vehicles; $\lambda = \frac{q}{(1 - t_m q)}$. If a vehicle reaches the right end of the road section, it will leave when the traffic light is green and will stop when the traffic light is red.

2.3 Traffic Safety Risks of Partially Disrupted Infrastructures

Earthquakes can cause bridge damage or even collapse, which will change the traffic patterns on the whole network. Both the damaged infrastructure and the traffic volume affect car crash frequencies. Whenever a bridge is under repair with partial blockage by providing limited traffic, it can be practically treated as a work zone with increased traffic safety risks (Yang et al. 2015). Poisson Regression is a basic but popular count-data model to simulate traffic crash frequency. If historical crash data is available, statistical analyses with more advanced models (e.g., Negative Binomials, panel data models) can be conducted to capture the site-specific safety performance of the area. If the site-specific crash data is not available or sufficient, Poison model will be an ideal option as the default and baseline analysis model

thanks to its minimum data requirement and popularity. In a Poison regression model, the probability of road i having y_i crashes (where y_i is a non-negative integer) is given by

$$P(y_i) = \frac{EXP(-\lambda_i)\lambda_i^{y_i}}{y_i!} \tag{9}$$

where $P(y_i)$ is the probability of road i having y_i crashes per year and λ_i is the Poisson parameter for road i, which is equal to the expected number of crashes per unit time on road i, $E[y_i]$ (Washington et al. 2010). Poisson regression models are estimated by specifying the Poisson parameter λ_i (the expected number of events per period) as a function of explanatory variables. For the long-term recovery case, explanatory variables might include the average hourly traffic, length of roads, work zone length, and duration of work zone length. The most common relationship between explanatory variables and the Poisson parameters is the log-linear model,

$$\lambda_i = EXP(\beta x_i) \tag{10}$$

where x_i is the vector of explanatory variables and β is the vector of estimable parameters. In this formulation, the expected number of events per period is given by $E[y_i] = \lambda_i = EXP(\beta x_i)$ (Washington et al. 2010). According to Washington et al. (2010), this model is estimated by standard maximum likelihood methods, with the likelihood function given as

$$L(\beta) = \prod_i \frac{EXP[EXP(\beta x_i)][EXP(\beta x_i)]^{y_i}}{y_i!} \tag{11}$$

2.4 Resilience Index and Applications

2.4.1 Traffic Assignment

The static traffic assignment using user equilibrium (UE) model provides a reasonable and efficient prediction of the average travel time and is widely adopted by many transportation agencies and researchers. The mathematical formulation of UE can be given by

$$\text{Minimize} \quad \sum_i \int_0^{x_i} t_i(\omega)\, d\omega \tag{12}$$

subject to

$$x_i = \sum_r \sum_s \sum_k f_k^{rs} \delta_{i,k}^{rs}, \forall i \tag{13}$$

$$\begin{cases} \sum_k f_k^{rs} = q_{rs}, & \forall r, s \\ f_k^{rs} \geq 0, & \forall r, s \end{cases} \tag{14}$$

where x_i is the traffic flow on link i, $i \in link\ set\ A$; t_i is the travel time on link i; f_k^{rs} is the traffic flow on the k^{th} path connecting origin-destination (OD) pair $r-s$; $\delta_{i,k}^{rs}$ is the indictor variable: $\delta_{i,k}^{rs} = 1$, if link i is part of the k^{th} path connecting OD pair $r-s$, otherwise $\delta_{i,k}^{rs} = 0$. q_{rs} is the travel demand from r (origin) to s (destination) (Wardrop 1982).

2.4.2 System Resilience Index

The total system travel time (TSTT) is proposed to reflect the efficiency of the transportation network and is defined as

$$TSTT = \sum_i t_i(x_i) = \sum_i t_0 \left(1 + \alpha \left[\frac{x_i}{C_i}\right]^{\beta}\right) \tag{15}$$

where C_i is the traffic carrying capacity of link i; $t_0 \left(1 + \alpha \left[\frac{x_i}{C_i}\right]^{\beta}\right)$ is from the Bureau of Public Roads (BPR) function; α and β are BPR function parameters with classical values of 0.15 and 4.0, respectively (US Bureau of Public Roads 1964), but their values vary by link types according to recent studies (Hou et al. 2017, 2019). In this study, the travel demand stays the same during the long-term recovery period. So, the smaller TSTT's value is, the more efficient the network is in terms of travel time. The efficiency indicator of the system is defined as

$$R_t = \frac{TSTT_0}{TSTT} \tag{16}$$

where $TSTT_0$ and $TSTT$ are for the pre-disaster period and long-term recovery period respectively.

The expected total system crash frequency (TSCF) is used to quantify the traffic safety risk of the network, which is defined as:

$$TSCF = \sum_i \lambda_i \tag{17}$$

The safety indicator of the system is defined as:

$$R_s = \frac{TSCF_0}{TSCF} \tag{18}$$

where $TSCF_0$ and $TSCF$ are for the pre-disaster period and long-term recovery period respectively.

The resilience index (RI) in this study is proposed to consider both traffic efficiency and safety performance:

$$RI = m.R_t + (1 - m).R_s \tag{19}$$

where m is a weight parameter between [0, 1], which is usually defined by the stakeholders based on the specific scenario and priority.

2.5 System Reliability and Post-earthquake Restoration Prioritization

2.5.1 System Reliability

System reliability R is the probability that a system can maintain its functionality while suffering from some extent of disruption. It is an important performance indicator for hazard resilience since it can provide an estimation of the system serviceability including uncertainties and relative importance of different links in terms of resilience performance, which is defined as:

$$R(\varepsilon) = P(RI_M \geq \varepsilon) \tag{20}$$

where RI is the resilience index of the system; M is the size of the samples using heuristic method; ε is the level-of-performance (LOP) of the disrupted transportation network specified by stakeholders, and it is a ratio between 0 and 1 being used as a criterion to assess whether the reduced serviceability of the disrupted network is acceptable or not.

2.5.2 Resilience-based Post-earthquake Bridge Restoration Prioritization

Due to usually limited resources, it is important for decision makers to optimize the resources on pre-disaster preventive strengthening and post-hazard recovery efforts. Accordingly, the stakeholders often would need to know the priorities of bridges in terms of these preventive and recovery efforts before and after hazards. In addition, it is imperative to accommodate the uncertainties related to the seismic intensity, bridge fragility, travel time and safety during the assessment of the priorities. In this study, the restoration priority of a bridge is not only related to the importance of the bridge to the network, which means the difference between the performance indicators of the network when the bridge is intact, partially failed or totally failed, but also affected by the required repair time of the bridge. If a vulnerable bridge has a great impact on the network and takes relatively less time to repair, it should be prioritized during the restoration. When considering the priorities of different bridges under a given state, a rational way is to optimize the reconstruction sequence to maximize the resilience index Z over time:

$$\text{Maximize } Z = \int_0^T RI(t)dt \tag{21}$$

where Z is the integration of the resilience index over the recovery time; T is the total recovery time of the system which is defined as the sum of the repair times of all the damaged bridges.

The sequence rankings are direct indicators for the restoration priorities of bridges under a given state. Among the damaged bridges, the smaller a bridge's repair sequence ranking is, the higher prioritization the bridge would receive. Considering the uncertainties in earthquakes and bridge failures, it is important to apply the Monte Carlo Simulation or Latin Hypercube Sampling to generate possible damage states of the bridges and develop the repair sequences of different bridges under each generated state. The mean restoration sequence (MRS) of any bridge i considering uncertainties is defined as:

$$MRS_i = \frac{\sum_1^M Seq_{i,m}}{M}, m \in [1, M] \tag{22}$$

where MRS_i is the MRS of bridge i, M is the size of the samples using heuristic method, and $Seq_{i,m}$ is the restoration sequence of bridge i under scenario m. As discussed earlier, MRS incorporates the failure rates of different bridges. However, when planning the post-hazard restoration of damaged bridges with limited resources, it is more meaningful for stakeholders to know which bridge to repair first and then the next for any given damage scenario. Thus, it is necessary to eliminate the effect of bridge failure rate on MRS when deriving the post-hazard restoration priority of bridges.

Therefore, the bridge priority index is defined as:

$$PR_i = \frac{n*(1-Pf_i)}{MRS_i}\ ,\ Pf_i \in (0,1) \tag{23}$$

where PR_i is the post-hazard restoration priority index of bridge i, n is the number of bridges in the network, and Pf_i is the failure rate of bridge i. The bigger PR is, the more prioritized the bridge should be. The proposed PR is a comprehensive prioritization indicator related not only to the network topology and bridge locations but also to origin-destination matrix and bridge repair times.

3. CASE STUDY

3.1 Centerville Transportation Network

Figure 3.1 shows the basic traffic network of a virtual community called Centerville located in earthquake-prone areas (Ellingwood et al. 2016). Following existing studies on this virtual community, the earthquakes are with Richter Magnitude between 5 and 7.25, depth of 10 kilometers and epicenter longitude and latitude coordinates of [-97.20, 35.20]. Some basic information of the network is shown in Table 3.1 and the length of each link is calculated based on the geographic information of the community. There are 20 zones in the community. Each of the 20 nodes in Figure 3.1 is the center of a zone in the community. Most of the industry or companies are in the I zone (industrial areas); most of the schools, universities, markets, shopping centers and recreational facilities are in the P zones (Public areas); and most of the residents live in the R zones (residential areas). In this study, only bridge damages may cause the links to be totally or partially disrupted. Nine out of the thirty-three roads/links are therefore vulnerable to earthquakes due to the existence of bridges (*B1-B9*) on these links (marked in Figure 3.1). There are nine types of bridges in the community with: multi-span continuous (MSC) concrete, slab, and steel bridges; multi-span simple supported (MSSS) concrete girder, concrete box girder, steel girder and slab bridges; and simple supported (SS) concrete girder and steel girder bridges. The parameters in Table 3.1 are determined based on the link information and the parameters in Table 3.2 and Table 3.3 are derived from the microscopic traffic flow simulation model. When comparing Centerville's transportation network to real-world ones, it has the similar size as a small to medium sized city's transportation network. So, the population is assumed to be 120,000 based on the traffic capacity of the network.

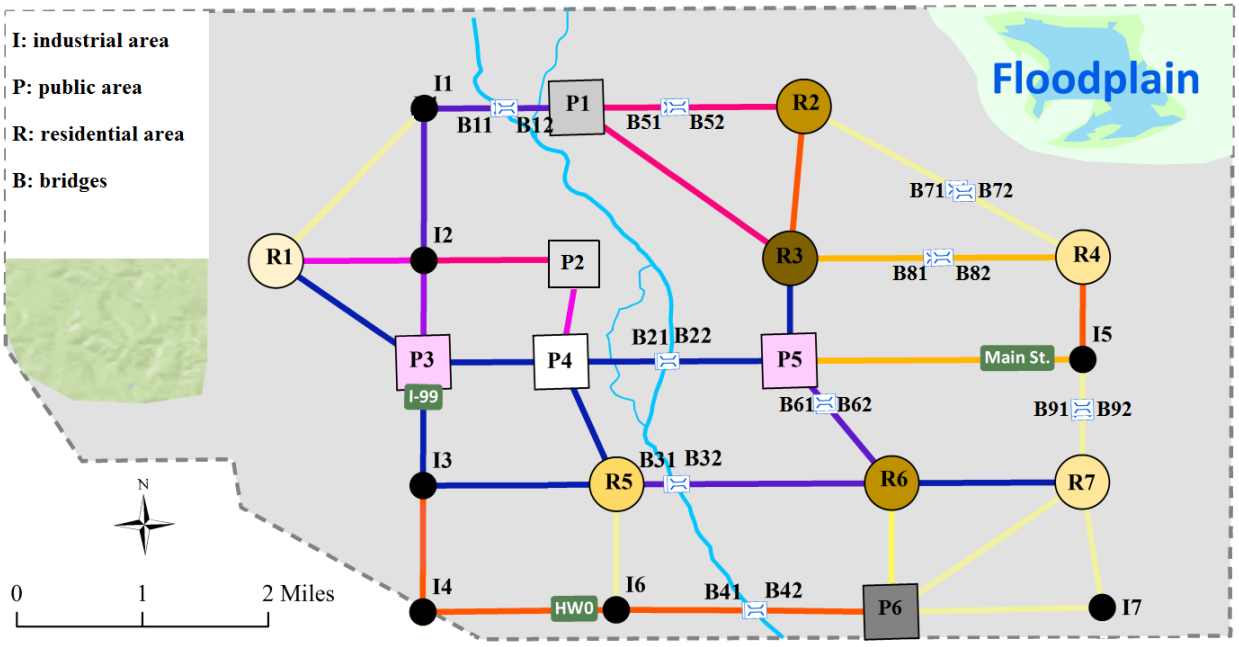

Figure 3.1 Transportation network of Centerville

Table 3.1 Link characteristics

Link#	Zone1	Zone2	Length (km)	No. of lanes	Bridges	Bridge longitudes	Bridge latitude
1	I1	I2	1.94	1	0		
2	I1	P1	1.59	1	MSC Concrete	-97.479543	35.256638
3	I1	R1	2.48	1	0		
4	I2	P2	1.62	1	0		
5	I2	P3	1.31	1	0		
6	I2	R1	1.55	1	0		
7	I3	I4	1.62	1	0		
8	I3	P3	1.57	1	0		
9	I3	R5	2.02	2	0		
10	I4	I6	2.02	1	0		
11	I5	P5	3.07	2	0		
12	I5	R4	1.31	1	0		
13	I5	R7	1.57	1	SS Steel	-97.461509	35.226897
14	I6	P6	2.88	1	MSSS concrete	-97.460889	35.212719
15	I6	R5	1.61	1	0		
16	I7	P6	2.21	1	0		
17	I7	R7	1.62	1	0		
18	P1	R2	2.38	1	MSSS conc box	-97.452268	35.197926
19	P1	R3	2.97	1	0		
20	P2	P4	1.32	2	0		
21	P3	P4	1.44	2	0		
22	P3	R1	2.03	1	0		
23	P4	P5	2.39	2	MSC Slab	-97.459936	35.256156
24	P4	R5	1.68	2	0		
25	P5	R3	1.31	2	0		
26	P5	R6	1.91	2	MSSS slab	-97.443390	35.221606
27	P6	R6	1.65	1	0		
28	P6	R7	2.58	1	0		
29	R2	R3	1.95	1	0		
30	R2	R4	3.52	1	MSSS steel	-97.427446	35.245770
31	R3	R4	3.07	1	SS concrete	-97.430203	35.237922
32	R5	R6	2.88	2	MSC Steel	-97.413721	35.220139
33	R6	R7	1.99	1	0		

Table 3.2 Estimated parameters of BPR functions for normal traffic

Link#	t_0 (min)	α	β	C (veh/h)
1	2.21	0.093	7.397	745
2	1.83	0.111	6.767	745
3	2.63	0.070	7.671	745
4	1.83	0.111	6.767	745
5	1.57	0.100	7.761	745
6	1.83	0.111	6.767	745
7	1.83	0.111	6.767	745
8	1.83	0.111	6.767	745
9	2.21	0.093	7.397	1490
10	2.21	0.093	7.397	745
11	3.11	0.052	8.054	1490
12	1.57	0.100	7.761	745
13	1.83	0.111	6.767	745
14	3.11	0.052	8.054	745
15	1.83	0.111	6.767	745
16	2.21	0.093	7.397	745
17	1.83	0.111	6.767	745
18	2.63	0.070	7.671	745
19	3.11	0.052	8.054	745
20	1.57	0.100	7.761	1490
21	1.57	0.100	7.761	1490
22	2.21	0.093	7.397	745
23	2.63	0.070	7.671	1490
24	1.83	0.111	6.767	1490
25	1.57	0.100	7.761	1490
26	2.21	0.093	7.397	1490
27	1.83	0.111	6.767	745
28	2.63	0.070	7.671	745
29	2.21	0.093	7.397	745
30	3.63	0.066	6.904	745
31	3.11	0.052	8.054	745
32	3.11	0.052	8.054	1490
33	2.21	0.093	7.397	745

Table 3.3 Estimated parameters of BPR functions for disrupted traffic

Link#	t_0 (min)	α	β	C (veh/h)
23	2.67	0.273	4.267	820
26	2.25	0.3063	4.344	820
32	3.15	0.2429	4.106	820

According to Eqs. (3-4), the peak ground acceleration (PGA) can be estimated using seismic attenuation laws. In this study, we employed the seismic attenuation law developed by Atkinson and Boore (1995). Their ground motion relation works for earthquakes of $4 \leq M_L \leq 7.25$ with epicentral depth of 10km and the mean PGA is estimated as:

$$\log(\text{PGA}) = \mathrm{c}_1 + \mathrm{c}_2(\mathrm{M}_L - 6) + \mathrm{c}_3(\mathrm{M}_L - 6)^2 - \log R_e - \mathrm{c}_4 R_e \tag{24}$$

where M_L is the Richter magnitude; R_e is the epicentral distance; c_1, c_2, c_3, and c_4 are parameters from regression analysis. According to the study by Atkinson and Boore (1995), $\mathrm{c}_1 = 3.79$, $\mathrm{c}_2 = 0.298$, $\mathrm{c}_3 = -0.0536$, $\mathrm{c}_4 = 0.00135$ are adopted here primarily for demonstration purposes. For a specific region with sufficient historical data, more site-specific parameters can be used after calibration. It is assumed in this study that M_L is a uniformly distributed random variable.

In Eq. (1), Nielson and DesRoches (2007) defined bridge fragility as the probability that the seismic demand meets or exceeds its capacity. The median PGA value med_i and dispersion ζ_i of different damage states are shown in Table 3.4.

Table 3.4 Median and dispersion values for seismic fragility curves of nine bridge classes (Nielson & DesRoches 2007)

Bridge Class	Median PGA Values (g)		Dispersion ζ_i
	Extensive med_i	Complete med_i	
MSC concrete	0.75	1.03	0.7
MSC slab	0.78	1.73	0.7
MSC steel	0.39	0.5	0.55
MSSS concrete	0.83	1.17	0.65
MSSS concrete box	1.19	2.92	0.75
MSSS slab	0.94	1.92	0.75
MSSS steel	0.56	0.82	0.5
SS concrete	2.62	3.64	0.9
SS steel	1.52	2.49	0.55

We take afternoon rush hour (5:00pm-6:00pm) as the study period. The origin-destination data is estimated by the Memphis travel demand model of Metropolitan Planning Organization (MPO) (Kimley-Horn et al., 2007). There are nine trip purposes including journey to work, home based school, home based university, home based shopping, home based social-recreational, home-based pickup/drop-off, home based other, non-home based work and non-home based non-work. Some of the travel demand information is presented in Table 3.5. The population of the Memphis area is around 1,000,000. In the Memphis MPO model (Kimley-Horn et al., 2007), a survey was conducted about the transportation modes of people's trips. About 99.8% of the trips are auto-based (drive alone, shared ride, bus, etc.). The

average occupancies of a shared ride and a bus are 2.4 and 7.2, respectively, according to Henao and Marshall (2019) and Federal Highway Administration (2018). The number of vehicle trips for every trip purpose of Centerville during the afternoon rush hour is estimated from the MPO model, assuming it has the same demographic properties as the Memphis area except population size. Table 3.6 lists the nine simplified trip purposes to fit the Centerville context. For any trip classification, if there are more than one origin-destination pairs, the trips will be evenly distributed between two different OD pairs due to the lack of enough information. Table 3.6 is based on people's typical trip behavior, e.g., journey to work trips is classified as trips from industrial areas to residential areas because "go home from work" is very typical during the afternoon rush hour. The origin-destination data is randomly assigned to different OD pairs based on the estimated trips among the residential, industrial, and public areas, and the related information is shown in Table 3.7.

Table 3.5 Memphis area travel demand information (Kimley-Horn et al., 2007)

Trip Purpose	Daily total trips	Intrazonal trip %	PM rush hour %
Journey to work	949,895	0.027	0.123
Home based school	334,407	0.056	0.044
Home based university	50,197	0.057	0.044
Home based shopping	199,141	0.101	0.086
Home based social recreational	218,306	0.056	0.086
Home based pickup/drop-off	182,627	0.074	0.086
Home based other	546,012	0.011	0.086
Non-home based work	122,174	0.075	0.037
Non-home based non-work	457,157	0.055	0.037

Table 3.6 Simplification of nine trip purposes

Trip Purpose	Trip origin and destination	Classification
Journey to work	work to home	Industrial to Residential
Home based school Home based university	public to home	Public to Residential
Home based shopping Home based social recreational	home to/from public	Residential to/from Public
Home based pickup/drop-off Home based other	Between home and any other places	Residential to/from residential, public, and industrial areas
Non-home based work	work to public	Industrial to Public
Non-home based non-work	intra public	Public to Public

Table 3.7 Origin (column 1)-destination (row 1) data of afternoon rush hour

	I1	I2	I3	I4	I5	I6	I7	P1	P2	P3	P4	P5	P6	R1	R2	R3	R4	R5	R6	R7
I1	0	1	0	0	0	1	0	5	5	3	4	5	2	101	98	103	81	90	113	95
I2	2	0	0	0	0	1	1	4	4	4	4	6	3	112	129	91	98	88	99	93
I3	0	0	0	1	0	0	0	5	5	5	4	3	3	68	118	91	109	109	88	82
I4	0	0	1	0	0	0	1	3	5	4	4	5	5	96	78	104	98	84	104	92
I5	1	0	0	0	0	0	0	3	5	4	5	4	6	102	123	105	101	81	76	86
I6	1	0	0	2	2	0	0	4	4	4	4	5	4	77	105	107	99	86	90	101
I7	0	1	0	0	1	0	0	4	4	3	6	5	5	89	90	95	90	60	89	103
P1	1	0	0	0	0	1	0	0	25	16	21	15	21	50	53	48	47	52	42	42
P2	2	1	0	0	1	0	1	31	0	28	22	26	19	31	46	47	47	35	35	31
P3	0	0	0	0	0	0	0	20	12	0	15	23	19	49	43	50	41	42	47	35
P4	0	0	0	0	0	1	1	19	24	13	0	13	14	39	49	45	40	46	32	46
P5	0	0	0	2	1	0	1	25	20	22	21	0	18	41	41	44	51	32	36	32
P6	0	1	1	1	2	1	0	23	16	32	24	18	0	53	40	47	41	45	35	45
R1	9	5	15	5	12	8	12	39	28	18	26	27	35	0	29	31	14	34	15	13
R2	8	9	10	3	8	9	12	39	37	27	29	30	32	18	0	4	23	25	22	20
R3	15	12	6	11	12	7	7	30	39	36	32	35	38	19	9	0	22	25	15	19
R4	8	10	13	10	10	5	6	37	35	33	32	30	25	16	19	11	0	19	13	26
R5	8	7	7	10	8	10	5	28	42	34	34	31	37	10	21	15	16	0	16	17
R6	5	4	8	11	6	9	11	42	30	26	28	40	29	18	17	20	25	16	0	18
R7	8	14	12	12	11	13	18	40	22	35	34	31	30	24	12	19	22	14	21	0

For the virtual community adopted in this study, the traffic crash data as well as detailed traffic volume data are not available. Without losing generality in the demonstration, the assumed observed number of traffic crashes (NTC) during afternoon rush hour over 1 year is shown in Table 3.8, where AHT is the average hourly traffic and it is from the traffic assignment of the OD matrix in Table 3.7; L_{wz} and t_{wz} are the length and the construction time of the work zone; L_{link} is the link length; and t_{ob} is the observation time (1 year for this case). Poisson regression (Eqs. (9-11)) analysis gives coefficients $\beta = -0.12754; 0.4382; 0.1449; 0.8198; 0.7548$ for *constant*, AHT, L_{link}, L_{wz}/L_{link} and t_{wz}/t_{ob}, respectively. In this study, it is assumed that there is no work zone in the pre-disaster period and the work zones during the long-term recovery period are only caused by the bridges suffering extensive and complete damage states which need repair. The ratios of bridge lengths to their link lengths are randomly generated between [0.05, 0.15].

Table 3.8 Parameters and observed number of crashes of the system

Link #	AHT (k)	L_{link}	L_{wz}/L_{link}	t_{wz}/t_{ob}	NTC(1 year)
1	0.250	1.945	0.037	0.547	2
2	0.993	1.594	0.078	0.139	2
3	0.204	2.482	0.659	0.149	3
4	0.062	1.625	0.556	0.258	2
5	0.529	1.312	0.254	0.841	3
6	0.143	1.548	0.760	0.254	3
7	0.042	1.621	0.028	0.814	2
8	0.687	1.574	0.351	0.244	2
9	0.486	2.023	0.305	0.929	4
10	0.200	2.023	0.612	0.350	3
11	0.341	3.065	0.636	0.197	3
12	0.855	1.312	0.149	0.251	2
13	0.385	1.574	0.392	0.616	3
14	0.423	2.882	0.356	0.473	3
15	0.543	1.605	0.517	0.352	3
16	0.269	2.207	0.567	0.831	4
17	0.376	1.620	0.604	0.585	3
18	0.350	2.376	0.221	0.550	3
19	0.766	2.969	0.544	0.917	6
20	0.338	1.324	0.524	0.286	2
21	1.521	1.441	0.130	0.757	4
22	0.666	2.032	0.095	0.754	3
23	1.750	2.391	0.399	0.380	5
24	0.640	1.680	0.768	0.568	4
25	1.702	1.312	0.272	0.076	3
26	0.943	1.908	0.468	0.054	3
27	0.545	1.651	0.179	0.531	3
28	0.480	2.584	0.601	0.779	5
29	0.228	1.949	0.204	0.934	3
30	0.104	3.519	0.405	0.130	2
31	0.403	3.065	0.559	0.569	4
32	0.608	2.881	0.713	0.469	4
33	0.598	1.992	0.767	0.012	3

With LOP $\varepsilon = 0.8$ and $m = 0.5$, Monte Carlo approach is used to simulate the PGA with 1,000,000 samples and Latin Hypercube sampling is adopted to simulate bridge damage states with 1,000 samples. Applying Eqs. (12-20) in Matlab 2020, the results are shown in Table 3.9 and Figure 3.2-Figure 3.4. It is found from Table 3.9 that the increase of the $TSTT$ in terms of percentage is like but a little less than the increase of $TSCF$ as compared to the respective pre-disaster values, $TSTT_0$ and $TSCF_0$. It is likely because traffic crashes are very sensitive to the presence of work zones, which is in accordance with the large coefficient values for L_{wz}/L_{link} and t_{wz}/t_{ob}. Figure 3.2-Figure 3.4 show that the post-hazard $TSTT$ and $TSCF$ for most sampled scenarios are concentrated within small ranges near $TSTT_0$ and $TSCF_0$

respectively and the system RI values are mostly close to 1. This phenomenon is mainly due to the low failure rate of the bridges when the Richter magnitude is low. In Figure 3.2, when TSTT is between 160 and 205, the cumulative distribution function (CDF) increases slowly. It may be because the failures of a certain bridge or specific combinations of bridges just have a very limited impact on the system travel time. If a vulnerable link has some alternative routes with similar travel time, its failure may not significantly impair the traffic efficiency of the system. Compared to Figure 3.2, Figure 3.3 has a smoother increase in the curve possibly because TSCF is very sensitive to the existence of work zones, which complies with the coefficient values of the Poisson regression. For instance, if some links as discussed above are partially closed, the system travel time doesn't increase considerably, but the number of traffic crashes may increase because of the existence of work zones. Figure 3.4(a) shows that CDF has almost no increase from 0.5-0.65 and 0.9-1, a slow increase from 0.65-0.8, a rapid increase from 0.8-0.9, and a dramatic increase at 1. Since the resilience index is based on both TSTT and TSCF, such phenomenon can be explained by the observed trends in the CDF curves of TSTT and TSCF. We fit the system resilience to various probability distributions and found out that Beta distribution had the best fit. Figure 3.4(b) shows Beta distribution fits the system resilience very well at most points. So, the Beta distribution may be used to estimate the system resilience.

Table 3.9 System indices

System index	Value
Pre-disaster $TSTT_0$ (min/hour)	150.85
Pre-disaster $TSCF_0$ (/year)	59.66
Post-hazard mean $TSTT$ (min/hour)	171.50
Post-hazard mean $TSCF$ (/year)	68.80
Increase in $TSTT$ (%)	13.69
Increase in $TSCF$ (%)	15.32
System reliability	0.85

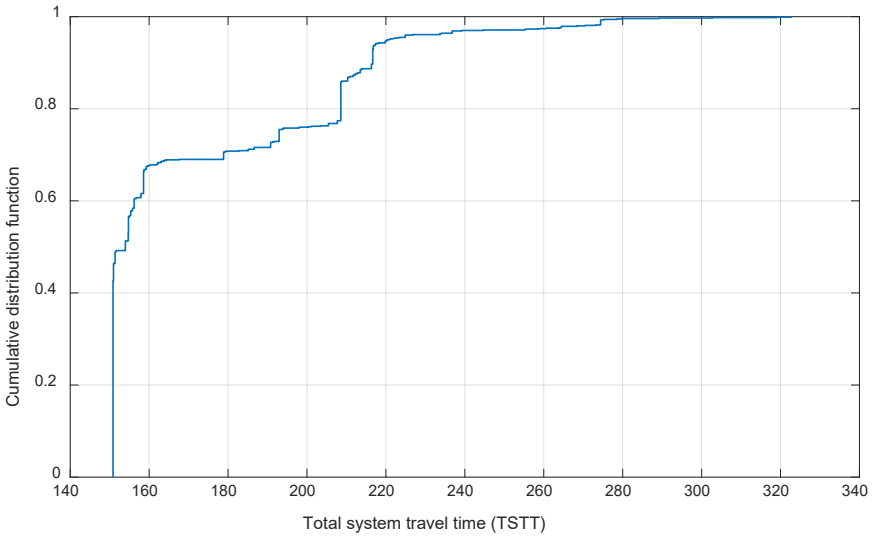

Figure 3.2 Cumulative distribution of TSTT

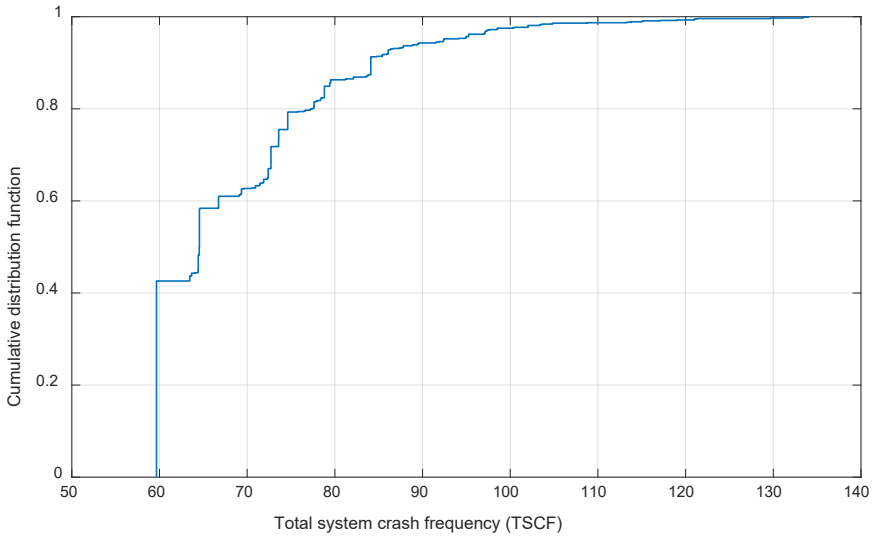

Figure 3.3 Cumulative distribution of TSCF

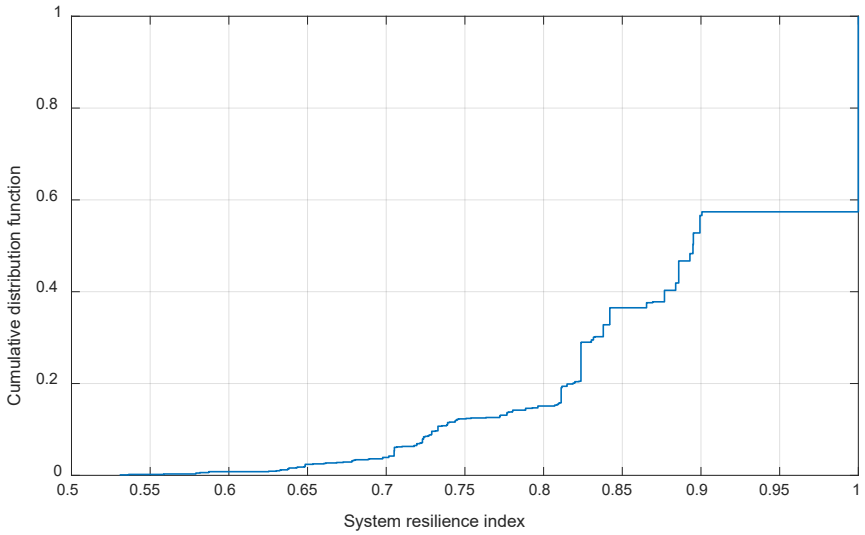

(a) Cumulative distribution of system resilience index

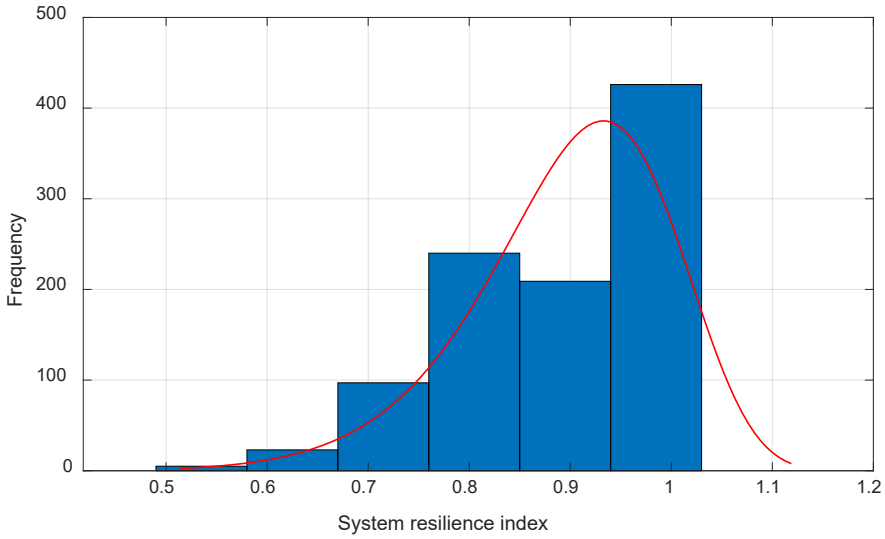

(b) Histogram of system resilience index

Figure 3.4 Distribution of system resilience index

The impacts of earthquake intensity and LOP on the system reliability are also studied and the results are presented in Figure 3.5 and Figure 3.6. It is found in Figure 3.5 that the system reliability R decreases more slowly at lower earthquake intensities, and then decreases more quickly but almost linearly at higher magnitudes. As expected, a stronger earthquake will cause a higher chance of damages on the bridges, and in turn, lower the system resilience index and reliability of the whole system. Apparently when the earthquake intensity is low, almost no bridge fails, which may be the reason for the slower drop in the system reliability at the lower magnitudes. In Figure 3.6, it is found that the system resilience index remains stable around 1 when the level-of-performance (LOP) is low. It is because the network remains a certain level of functionality, even under the worst bridge damage situations. So, the network meets the low LOP in almost all the sampled damage scenarios. Then system reliability slowly decreases when LOP is between 0.6-0.8. It is because some severely damaged scenarios can no longer meet the increasing

LOP. The failures of the most important bridges or bridge combinations happen during this interval, and the damage of any of these bridges or bridge combinations will greatly reduce the system performance. When the LOP is between 0.8-0.9, the system reliability quickly decreases, representing a deteriorating condition from the system resilience perspective. It means when the LOP is high, the network with failures of even a very limited number of bridges or a certain bridge that have limited importance to the network performance cannot meet the performance criterion. The selection of LOP value in this interval will ensure the network doesn't suffer any major damage and remains a very high level of functionality. So, it is the reasonable interval for LOP values.

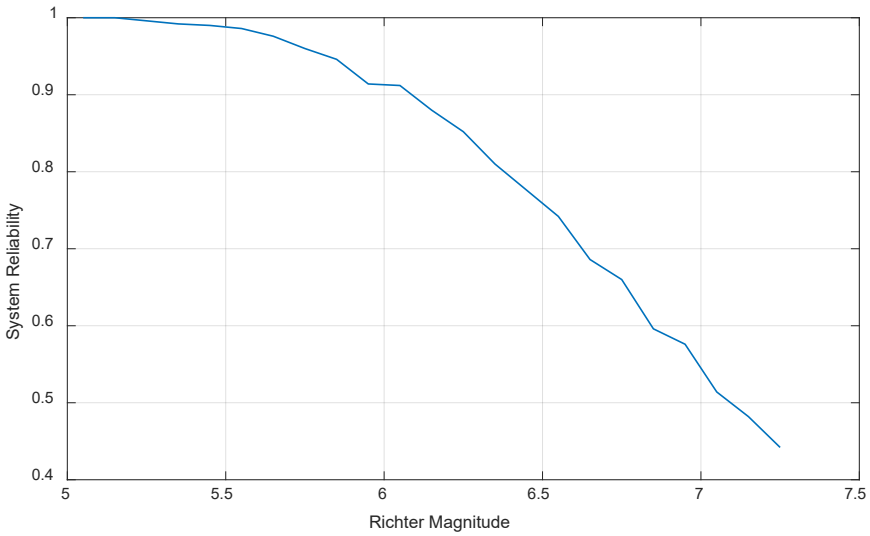

Figure 3.5 System reliability as a function of Richter magnitude

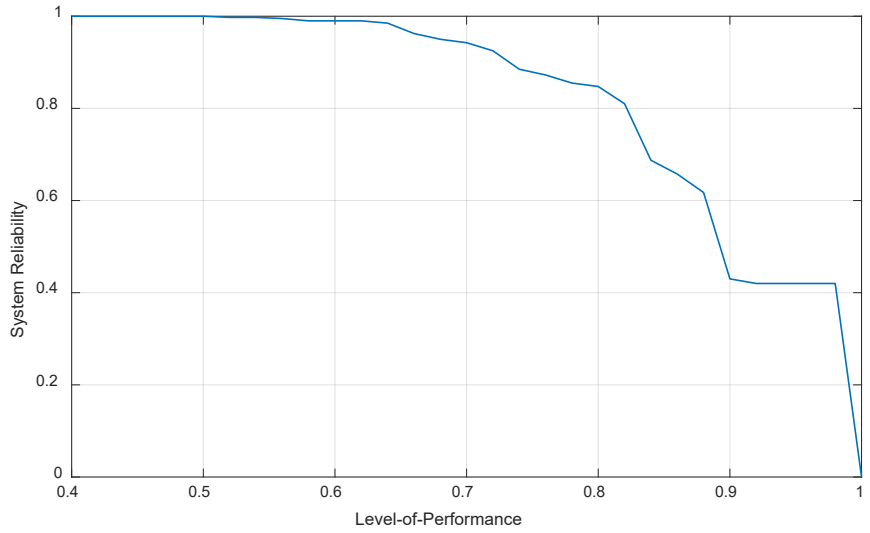

Figure 3.6 System reliability as a function of level-of-performance

3.2 Post-earthquake Bridge Restoration Prioritization

Due to the relatively low failure rates for bridges, none or just few of the bridges are damaged in most of the possible states generated from Latin Hypercube sampling. In this case, we would restore the damaged (extensive damage or higher) bridges in the best sequences while the restoration sequences of fully functional (lower than extensive damage) bridges are set to be the last. There is a total of 9 bridges in the network. Assuming the repair time for bridges B1 to B9 are 98, 74, 99, 90, 79, 83, 85, 97, and 77 days respectively if they are damaged, the optimization is based on Eqs. (21-23) and is derived from the Greedy Algorithm, and the result is presented in Figure 3.7. It is found that Bridge 9 on link (I5, R7) has the highest priority due to the network topology, bridge location, etc. From Figure 3.1 and Table 3.2, we can tell Bridge 9 is very important to trips between OD pairs including (I5, R7), (R4, R7), (I5-I7), (P6, I5), (P6, R4), (I7, R4) and so on. All these trips don't have alternatives with similar travel time. Among these OD pairs, (I5, R7), (P6, R4), (I7, R4), and (R4, R7) have considerable number of trips. A great increase in the travel time and the number of traffic crashes can be expected when Bridge 9 suffers extensive or complete damages. Similarly, Bridge 7 has the least priority because of the relatively insignificant location in the graph in terms of travel time and safety. Figure 3.1 and Table 3.2 show Bridge 7 is significant to trips between (R2, R4) and has some impact on trips between (I5, R2) and (R2, R7). The travel demand between (R2, R4) is not big and the trips between (I5, R2) and (R2, R7) don't rely on link (R2, R4) too much. For trips that need to go between P1 and R4, link (R2, R4) is not an essential choice because an efficient alternative route is available, say (P1-R3-R4).

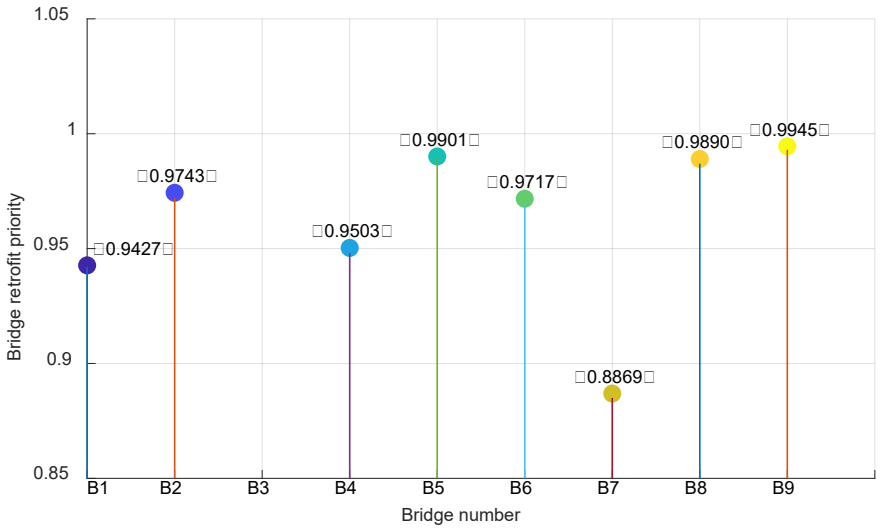

Figure 3.7 Post-hazard restoration priority for different bridges

4. CONCLUSIONS AND DISCUSSIONS

Long-term recovery is a very important stage following any major hazard or incident. A framework of modeling resilience-related performance of a transportation network was developed from both travel time and traffic safety perspectives. In the model, uncertainties in the earthquake information and fragility of the bridges were addressed to simulate real-world earthquake scenarios and possible disconnected or partial functioning bridges. A resilience performance indicator was introduced to evaluate the overall travel time and safety performance for the whole network and a bridge restoration prioritization index was proposed to evaluate the relative restoration priorities of different bridges in a traffic network. The priority information of bridges can help developing more efficient post-hazard long-term recovery strategy by keeping those bridges robust and functional in the long-term recovery stage. Based on the long-term recovery performance in terms of travel time and safety, the proposed model can assist on developing rational long-term recovery plan for a community with some partially functional bridges. Finally, the proposed framework was demonstrated in a hypothetical community located in earthquake-prone areas and is at the risk of extensive earthquake attacks. This study has two main innovative contributions: (1) simulating the traffic performance of partially closed road segments in the network simulation and optimization, which offer useful tool to capture the time-progressive recovery process; and (2) integrating both traffic efficiency and safety into the resilience assessment and recovery prioritization. Despite the approximations and relatively simpler models being adopted, it is noted that the proposed approach is general enough to be extended to more advanced models with more site-specific data without losing generality.

This study, however, also has some limitations. The traffic crash frequency was estimated with Poisson model due to the popularity, simplicity, and low requirement of site-specific data. There are some more advanced traffic crash frequency modeling techniques which can be applied in the proposed framework when more actual historical crash data are available for parameter calibrations to consider site-specific characteristics. Also, due to the lack of data and computation complexity, we didn’t consider the deterioration effect (García-Segura et al., 2017) of bridges and the interdependency between the transportation network and other lifeline systems, which are also important for studying community resilience.

Following the same methodology, more specific study on a community with realistic data can be conducted in the future. For potential future study, more advanced traffic safety modeling techniques like Negative Binomial model and comprehensive site-specific traffic accident data will be applied to estimate the community's traffic crash frequency. Dynamic traffic assignment algorithms will be used to model the change of travel demand and traffic flow during a day instead of just focusing on the traffic performance during the afternoon rush hour. Infrastructure deterioration effect and interdependency among different lifeline systems will be considered to make the simulation more sophisticated and accurate.

REFERENCES

Adachi, T., & Ellingwood, B. (2007). Impact of infrastructure interdependency and spatial correlation of seismic intensities on performance assessment of a water distribution system. In *Proceedings of the 10th International Conference on Applications of Statistics and Probability in Civil Engineering*.

Akcelik, R. (1996). Relating flow, density, speed and travel time models for uninterrupted and interrupted traffic. *Traffic Engineering+ Control*, *37*(9), 511-16.

Akiyama, M., Frangopol, D. M., & Ishibashi, H. (2020). Toward life-cycle reliability-, risk-and resilience-based design and assessment of bridges and bridge networks under independent and interacting hazards: emphasis on earthquake, tsunami and corrosion. *Structure and Infrastructure Engineering*, *16*(1), 26-50.

Alipour, A., & Shafei, B. (2016). Seismic resilience of transportation networks with deteriorating components. *Journal of Structural Engineering*, *142*(8), C4015015.

Argyroudis, S. A., Mitoulis, S. A., Hofer, L., Zanini, M. A., Tubaldi, E., & Frangopol, D. M. (2020). Resilience assessment framework for critical infrastructure in a multi-hazard environment: Case study on transport assets. *Science of The Total Environment*, *714*, 136854.

Argyroudis, S. A., Mitoulis, S. A., Winter, M. G., & Kaynia, A. M. (2019). Fragility of transport assets exposed to multiple hazards: State-of-the-art review toward infrastructural resilience. *Reliability Engineering & System Safety*, *191*, 106567.

Atkinson, G. M., & Boore, D. M. (1995). Ground-motion relations for eastern North America. *Bulletin of the Seismological Society of America*, *85*(1), 17-30.

Blackman, D., Nakanishi, H., & Benson, A. M. (2017). Disaster resilience as a complex problem: Why linearity is not applicable for long-term recovery. *Technological Forecasting and Social Change*, *121*, 89-98.

Bocchini, P., & Frangopol, D. M. (2012a). Restoration of bridge networks after an earthquake: Multicriteria intervention optimization. *Earthquake Spectra*, *28*(2), 426-455.

Bocchini, P., & Frangopol, D. M. (2012b). Optimal resilience-and cost-based postdisaster intervention prioritization for bridges along a highway segment. *Journal of Bridge Engineering*, *17*(1), 117-129.

Campbell, K. W. (1981). Near-source attenuation of peak horizontal acceleration. *Bulletin of the Seismological Society of America*, *71*(6), 2039-2070.

Chang, L., Peng, F., Ouyang, Y., Elnashai, A. S., & Spencer Jr, B. F. (2012). Bridge seismic retrofit program planning to maximize postearthquake transportation network capacity. *Journal of Infrastructure Systems*, *18*(2), 75-88.

Chang, L., Elnashai, A. S., & Spencer Jr, B. F. (2012). Post-earthquake modelling of transportation networks. *Structure and infrastructure Engineering*, *8*(10), 893-911.

Chang, S. E., & Nojima, N. (2001). Measuring post-disaster transportation system performance: the 1995 Kobe earthquake in comparative perspective. *Transportation Research Part A: Policy and Practice*, *35*(6), 475-494.

Chen, Y. W., & Tzeng, G. H. (1999). A fuzzy multi-objective model for reconstructing the post-quake road-network by genetic algorithm. *International Journal of Fuzzy Systems*, *1*(2), 85-95.

Cho, S., Gordon, P., Richardson, H. W., Moore, J. E., & Shinozuka, M. (2000). Analyzing transportation reconstruction network strategies: a full cost approach. *Review of Urban & Regional Development Studies*, *12*(3), 212-227.

Dong, Y., & Frangopol, D. M. (2015). Risk and resilience assessment of bridges under mainshock and aftershocks incorporating uncertainties. *Engineering Structures*, *83*, 198-208.

El-Anwar, O., Ye, J., & Orabi, W. (2015). Efficient optimization of post-disaster reconstruction of transportation networks. *Journal of Computing in Civil Engineering*, *30*(3), 04015047.

El-Anwar, O., Ye, J., & Orabi, W. (2015). Innovative linear formulation for transportation reconstruction planning. *Journal of Computing in Civil Engineering*, *30*(3), 04015048.

Ellingwood, B, Cutler, H., Gardoni, P., Peacock, W., van de Lindt, J. and Wang, N. (2016). "The Centerville virtual community: a fully integrated decision model of interacting physical and social infrastructure systems", *Journal of Sustainable and Resilient Infrastructure*, 1, 3-4, 95-107.

Federal Highway Administration. (2018). Average Vehicle Occupancy Factors for Computing Travel Time Reliability Measures and Total Peak Hour Excessive Delay Metrics. Retrieved from https://www.fhwa.dot.gov/tpm/guidance/avo_factors.pdf

Frank, M., & Wolfe, P. (1956). An algorithm for quadratic programming. *Naval research logistics quarterly*, *3*(1-2), 95-110.

García-Segura, T., Yepes, V., & Frangopol, D. M. (2017). Multi-objective design of post-tensioned concrete road bridges using artificial neural networks. *Structural and Multidisciplinary Optimization*, *56*(1), 139-150.

Henao, A., & Marshall, W. E. (2019). The impact of ride-hailing on vehicle miles traveled. *Transportation*, *46*(6), 2173-2194.

Hou, G., Chen, S., Zhou, Y., & Wu, J. (2017). Framework of microscopic traffic flow simulation on highway infrastructure system under hazardous driving conditions. *Sustainable and Resilient Infrastructure*, *2*(3), 136-152.

Hou, G., & Chen, S. (2019). An Improved Cellular Automaton Model for Work Zone Traffic Simulation Considering Realistic Driving Behavior. *Journal of the Physical Society of Japan*, *88*(8), 084001.

Hu, Z. H., Sheu, J. B., & Xiao, L. (2014). Post-disaster evacuation and temporary resettlement considering panic and panic spread. *Transportation research part B: methodological*, *69*, 112-132.

Janson, B. N. (1991). Dynamic traffic assignment for urban road networks. *Transportation Research Part B: Methodological*, *25*(2-3), 143-161.

Kameshwar, S., Misra, S., & Padgett, J. E. (2020). Decision tree based bridge restoration models for extreme event performance assessment of regional road networks. *Structure and Infrastructure Engineering*, *16*(3), 431-451.

Kilanitis, I., & Sextos, A. (2019). Impact of earthquake-induced bridge damage and time evolving traffic demand on the road network resilience. *Journal of traffic and transportation engineering (English edition)*, *6*(1), 35-48.

Kimley-Horn and Associates, Inc., Cambridge Systematics, Inc., and HNTB. "Technical Memorandum: Memphis Travel Demand Model" *Prepared for Memphis MPO*, 2007.

Kozin, F., & Zhou, H. (1990). System study of urban response and reconstruction due to earthquake. *Journal of Engineering Mechanics*, *116*(9), 1959-1972.

Kucharski, R., & Drabicki, A. (2017). Estimating Macroscopic Volume Delay Functions with the Traffic Density Derived from Measured Speeds and Flows. *Journal of Advanced Transportation*, *2017*.

Lee, C., & Machemehl, R. B. (2005). *Combined traffic signal control and traffic assignment: algorithms, implementation and numerical results*. Southwest Region University Transportation Center, Center for Transportation Research, University of Texas at Austin.

Lipton, E. (2010). Devastation, Seen From a Ship. *New York Times*.

Liu, L., Yang, D. Y., & Frangopol, D. M. (2020). Network-level risk-based framework for optimal bridge adaptation management considering scour and climate change. *Journal of Infrastructure Systems*, *26*(1), 04019037.

Lu, X., Cheng, Q., Xu, Z., Xu, Y., & Sun, C. (2019). Real-time city-scale time-history analysis and its application in resilience-oriented earthquake emergency responses. *Applied Sciences*, *9*(17), 3497.

Liu, Y., McNeil, S., Hackl, J., & Adey, B. T. (2020). Prioritizing transportation network recovery using a resilience measure. *Sustainable and Resilient Infrastructure*, 1-12.

Merschman, E., Doustmohammadi, M., Salman, A. M., & Anderson, M. (2020). Postdisaster decision framework for bridge repair prioritization to improve road network resilience. *Transportation research record*, *2674*(3), 81-92.

Nielson, B. G., & DesRoches, R. (2007). Analytical seismic fragility curves for typical bridges in the central and southeastern United States. *Earthquake Spectra*, *23*(3), 615-633.

Orabi, W., El-Rayes, K., Senouci, A. B., & Al-Derham, H. (2009). Optimizing postdisaster reconstruction planning for damaged transportation networks. *Journal of Construction Engineering and Management*, *135*(10), 1039-1048.

Orabi, W., Senouci, A. B., El-Rayes, K., & Al-Derham, H. (2010). Optimizing resource utilization during the recovery of civil infrastructure systems. *Journal of management in engineering*, *26*(4), 237-246.

Padgett, J. E., & DesRoches, R. (2009). Retrofitted bridge fragility analysis for typical classes of multispan bridges. *Earthquake Spectra*, *25*(1), 117-141.

Padgett, J. E., & DesRoches, R. (2007). Bridge functionality relationships for improved seismic risk assessment of transportation networks. *Earthquake Spectra*, *23*(1), 115-130.

Sun, W., Bocchini, P., & Davison, B. D. (2020). Resilience metrics and measurement methods for transportation infrastructure: the state of the art. *Sustainable and Resilient Infrastructure*, *5*(3), 168-199.

US Bureau of Public Roads. Office of Planning. Urban Planning Division. (1964). *Traffic Assignment Manual for Application with a Large, High Speed Computer*. US Department of Commerce.

Wakabayashi, H., & Kameda, H. (1992). Network performance of highway systems under earthquake effects: A case study of the 1989 Loma Prieta earthquake. In *Proceedings of the US-Japan Workshop on Earthquake Disaster Prevention for Lifeline Systems. Tsukuba Science City, Japan* (Vol. 215232).

Wang, Z., & Jia, G. (2019). Efficient sample-based approach for effective seismic risk mitigation of transportation networks. *Sustainable and Resilient Infrastructure*, 1-16.

Wardrop, J. G. (1982). Some theoretical aspects of road traffic research. *Proceedings of the Institute of Civil Engineers*, (Part II), 325-378.

Washington, S. P., Karlaftis, M. G., & Mannering, F. (2010). *Statistical and econometric methods for transportation data analysis*. Chapman and Hall/CRC.

Wu, Y., & Chen, S. (2019). Resilience modeling of traffic network in post-earthquake emergency medical response considering interactions between infrastructures, people, and hazard. *Sustainable and Resilient Infrastructure*, *4*(2), 82-97.

Yang, H., Ozbay, K., Ozturk, O., & Xie, K. (2015). Work zone safety analysis and modeling: a state-of-the-art review. *Traffic injury prevention*, *16*(4), 387-396.

Yi, F., & Tu, Y. (2018). An evaluation of the paired assistance to disaster-affected areas program in disaster recovery: The case of the Wenchuan earthquake. *Sustainability*, *10*(12), 4483.

Zamanifar, M., & Seyedhoseyni, S. M. (2017). Recovery planning model for roadways network after natural hazards. *Natural Hazards*, *87*(2), 699-716.

Zhang, W., & Wang, N. (2016). Resilience-based risk mitigation for road networks. *Structural Safety*, *62*, 57-65.

Zhao, T., & Zhang, Y. (2020). Transportation infrastructure restoration optimization considering mobility and accessibility in resilience measures. *Transportation Research Part C: Emerging Technologies*, *117*, 102700.

Zhou, Y., Wang, J., & Sheu, J. B. (2019). On connectivity of post-earthquake road networks. *Transportation Research Part E: Logistics and Transportation Review*, *123*, 1-16.